Advances in Applied Mathematics and Mechanics
Adv. Appl. Math. Mech., Vol. 7, No. 5, pp. 625-643

DOI: 10.4208/aamm.2014.m517
October 2015

Numerical Analysis of Damage Thermo-Mechanical Models

Hamdi Hentati[1,*], Ilyes Ben Naceur[2], Wassila Bouzid[2]
and Aref Maalej[1]

[1] *LASEM Laboratory, National School of Engineers of Sfax, University of Sfax, Tunisia*
[2] *Unit of Mechanical Production and Materials, National School of Engineers of Sfax, University of Sfax, Tunisia*

Received 27 February 2014; Accepted (in revised version) 9 October 2014

Abstract. In this paper, we present numerical computational methods for solving the fracture problem in brittle and ductile materials with no prior knowledge of the topology of crack path. Moreover, these methods are capable of modeling the crack initiation. We perform numerical simulations of pieces of brittle material based on global approach and taken into account the thermal effect in crack propagation. On the other hand, we propose also a numerical method for solving the fracture problem in a ductile material based on elements deletion method and also using thermo-mechanical behavior and damage laws. In order to achieve the last purpose, we simulate the orthogonal cutting process.

AMS subject classifications: 65M10, 78A48

Key words: Fracture mechanics, brittle and ductile materials, variational approach, Johnson and Cook laws, and orthogonal cutting.

---

1 Introduction

The behavior of materials can be classified into two categories: brittle and ductile. So, steel and aluminum are usually fall in the class of ductile materials; glass and ceramic are fall in the class of brittle materials. These two categories can be distinguished by comparing the stress-strain curves. The material response for ductile and brittle materials are exhibited by both qualitative and quantitative differences in their respective stress-strain curves. Ductile materials will withstand large strains before the specimen rupture and the rupture in brittle materials fracture occurs at much lower strains. The yielding

*Corresponding author.
Email: hamdi.hentati@yahoo.fr (H. Hentati)

region for ductile materials often takes up the majority of the stress-strain curve, whereas for brittle materials it is nearly nonexistent.

The developments related to the theory of brittle fracture are based on the ideas of Griffith [1]. In this theory, the fundamental quantities are the toughness G_c and the energy release rate G. Propagation will take place if $G \geq G_c$. Despite the important contribution of this theory, it has some shortcomings detailed in [2, 3]. Recently, the fracture mechanics has been revisited by proposing different models of brittle fracture in linearly elastic bodies inspired from the Griffith's criterion. A variational theory was developed by Bourdin et al. [2] end was studied by [3–5] aiming to model brittle fracture. Then, for any displacement and crack configuration, one defines the total energy:

$$E(u,\Gamma) = P(e(u)) + G_c H^{N-1}(\Gamma), \tag{1.1}$$

where $P(e(u))$ denotes the elastic energy of the considered system subject to a displacement u and cracked along Γ. $H^{N-1}(\Gamma)$ denotes the $N-1$ dimensional Hausdorff measure of Γ, i.e., its length in 2D and its surface area in 3D. $e(u)$ is the strain field. In order to simulate the crack propagation based on the variational theory, we employ a numerical method using the alternate minimization algorithm. Therefore, the first objective of our work is to present the mains computational results of the crack initiation and propagation based on the variational approach and using an alternate minimization algorithm. In addition, we examine also the crack formation under thermal shock in brittle material, these numerical results will compared with experimental ones.

On the other hand and in order to propose a numerical method for solving the fracture problem in a ductile material, we simulate the orthogonal cutting of the ductile material by the formation of the discontinuous chip.

Cut modeling is highly conditioned by the relevance of the behavior law which should describe the main phenomena and their interactions. The Johnson and Cook law [6], presented in Eq. (1.2), is used to model orthogonal cutting.

$$\sigma_{eq} = [A + B\varepsilon^n]\Big[1 + C\ln\Big(\frac{\dot{\varepsilon}}{\dot{\varepsilon}_0}\Big)\Big]\Big[1 - \Big(\frac{T - T_{amb}}{T_f - T_{amb}}\Big)^m\Big], \tag{1.2}$$

T_f is the melting temperature, T_{amb} is the room temperature and T is the cutting temperature. A is the yield strength of the work material at room temperature. B and n represent the effects of strain hardening. C is the strain rate constant and m is the thermal softening fraction. The strain rate $\dot{\varepsilon}$ is normalized with a reference strain rate $\dot{\varepsilon}_0 = 1\text{s}^{-1}$. The continuous chip is characterized by a process of plastic deformation in the primary shear zone (see Fig. 1). The chip flows continuously. This configuration is the most modeled in the literature. One used two different methods to simulate the formation of the continuous chip. The first consists in predefining the geometry of the chip [7–9]. The second starts from an arbitrary geometry (i.e., without predefine the geometry of the chip) [10–14].

On the other hand, the discontinuous chip is characterized by its periodic rupture and by the appearance of cracks. The shear stress reaches the limit of the material break

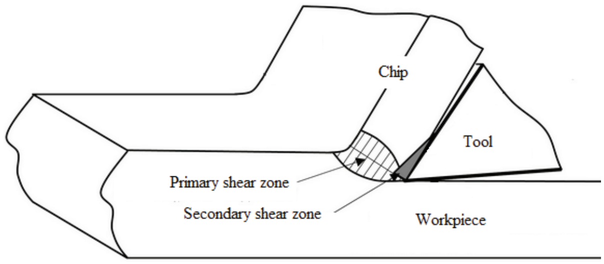

Figure 1: Primary shear zone location.

in the primary shear zone and a crack propagates. Starting from an arbitrary geometry (i.e., without predicted geometry of the chip), it is necessary to define a criterion for separation to simulate the formation of discontinuous chip. Therefore, the second goal of this paper is to present the behavior law and the failure model of Johnson and Cook to simulate the orthogonal cutting process. In fact, we describe some numerical methods to simulate orthogonal cutting with continuous and discontinuous chip and using the Johnson and Cook law to model the behavior of the workpiece material. We show two methods to modeling the formation of chip and to simulating the crack propagation in a ductile material: the elements deletion method and the Johnson and Cook damage model.

2 Overview of modeling the fracture mechanics

2.1 Fracture mechanics in fragile materials

The main objective of fracture mechanics is to determine the crack propagation in a continuous medium. The model of linear elasticity is sufficiently known to allow the study of brittle fracture in fragile materials such as ceramics and glass. The developments related to the theory of brittle fracture are mainly based on the ideas of Griffith [1]. He associates with each crack a surface energy proportional to its length. In this theory, the fundamental quantities are the toughness G_c and the energy release rate G. Consider a crack with length a in a deformable domain. For an ideally brittle material and according to the law of conservation of energies, the energy balance during crack growth takes the form:

$$G=\frac{\partial W}{\partial a}-\frac{\partial E_{elast}}{\partial a}=\frac{\partial E_{surf}}{\partial a}. \tag{2.1}$$

The cracks growth if $G \geq G_c$, and will not if $G < G_c$. The theory of Griffith [1] has some shortcomings detailed in [2,3]. So, the fracture mechanics has been revisited and authors propose other models of brittle fracture inspired from the Griffith's criterion.

A variational theory was developed by Francfort and Marigo [15], and was be used aiming to model brittle fracture [4,5,16–21]. The main idea consists in introducing a new

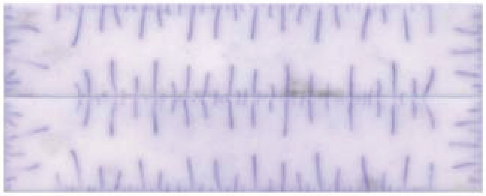

Figure 2: Crack pattern in a slab after a thermal shock (see [28]).

variable α as defined in functional of Ambrosio and Tortorelli [22,23] on image segmentation problems developed by Mumford and Shah [24]. This variable controls the damage of the structure. This theory allows the treatment of crack as surface of free discontinuity which takes place in a structure in such a way that the crack is maintained at a minimum level of the structure energy. The new functional characterizes the variational approach, is parameterized by η and is defined by the Eq. (2.2)

$$E(u,\alpha)=\frac{\mu}{2}\int\big((1-\alpha)^2+\epsilon(\eta)\big)\nabla u\cdot\nabla u dx+G_c\int\Big(\frac{\alpha^2}{4\eta}+\eta\nabla\alpha\cdot\nabla\alpha\Big)dx, \tag{2.2}$$

where u is the anti-plane displacement, the variable α controls the damage field of the structure, η is a regularized numerical parameter, ϵ is a positive infinitesimal whose role is to render coercive the regularized functional and μ is the shear modulus of the considered material. In this formulation (Eq. (2.2)), the energy is made of two parts. The first one is equal to the elastic energy, while the second is proportional to the crack length. In order to simulate the crack propagation based on the variational theory, the finite element method cannot predict the evolution of crack since it is unable to treat the space-time trajectories of crack. To overcome this difficulty, we employ a numerical method based on alternate minimization algorithm. In fact, The functional $E(u,\alpha)$ is not convex; this makes the research for a minimum of the energy a very complex task. However, this functional is convex at each variable separately, displacement u and damage variable α, and can therefore be iteratively minimized with respect to these variables.

On the other hand, we focus also on the crack propagation in brittle materials under thermal shock. The theoretical and numerical aspects of this problem have been studied by many authors using the Griffith theory. In this context, [25] discusses the initiation and propagation of the periodic crack pattern using a stress criterion for initiation. More recently, [26,27] study spacing and initiation by global minimization of the Griffith energy. Bourdin et al. [28] report numerical results of thermal shock problem obtained trough the variational approach, focusing on the spacing between cracks as a function of the depth (Fig. 2).

2.2 Fracture mechanics in ductile material

Because of the trend in the industry to optimise the cutting conditions and higher stroke rates, modelling of machining process requires the development of advanced material

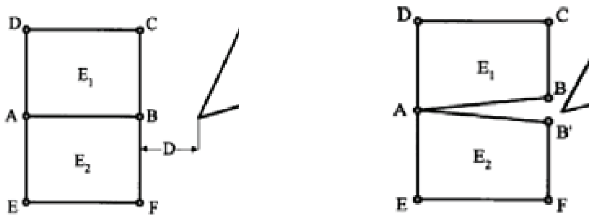

Figure 3: Nodal release procedure.

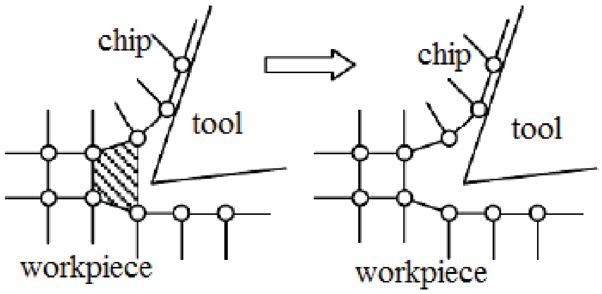

Figure 4: Deleting elements method.

models. Large plastic strain, hight strain rate and temperature effects, as well as damage and fracture have to be taken into account. Several models exist and can be characterized by different criteria, such as validity domain, physical or phenomenological bases, coupled or uncoupled. In the field of machining and forming processes, the more commonly used models are [6, 29–32]. Without going into details of these approaches, we are interesting for the Johnson and Cook model [6]. The purely phenomenological Johnson and Cook model is known for its simplicity and its ability to model hight strain rate processes with heating effect. The damage behavior is modeled by a critical strain fracture criterion. This damage model of Johnson and Cook may be used to simulate the formation of chip in machining process.

On the other hand, in literature, the simulation of the formation of discontinuous chip uses one of two criteria presented as follow:

- The chip segmentation is achieved through a nodal release procedure by defining a bonded interface along the cutting path and by applying the proposed segmentation criterion to the state at a fixed distance ahead of the tool edge (Fig. 3). The idea is to separate the chip from the workpiece when the distance D between the tool edge and the nearest node is less than a critical distance D_c.
- Deletion criterion of elements [13, 33]. Models based on the deleting elements method (Fig. 4) are similar to models based on nodal release procedure.

Thus, cracks can be created from the definition of the cutting model [34]. The crack propagates in elements in contact with the tool as a function of the feed of the latter up to the deletion of these elements. Other studies, as shown in [35], ones have defined a damage coefficient for chip breaking.

On the other hand, [14,34] are interest to Johnson and Cook law to model fracture in which, the model is based on the critical parameter $W_{JC}=\sum(\Delta\varepsilon_{eq}/\varepsilon_r)$.

$$\varepsilon_r=\Big[D_1+D_2\exp\Big(D_3\frac{\sigma_H}{\sigma_{eq}}\Big)\Big]\Big[1+D_4\ln\Big(\frac{\dot{\varepsilon_{eq}}}{\dot{\varepsilon}_0}\Big)\Big]\Big[1+D_5\Big(\frac{T-T_{amb}}{T_f-T_{amb}}\Big)^m\Big]. \tag{2.3}$$

The fracture will occur when the critical parameter of Johnson and Cook damage model [6] is $W_{JC}=1$. This model can take into account the effects of stress, the strain and temperature on the damage. The problem of this model is the identification of its parameters (D_1 to D_5).

3 Mechanical model of brittle fracture using the global approach

We assume that the material is elastic, isotropic and homogeneous with shear modulus μ. The static model of anti-plane shear with fracture is given by minimizing the regularized energy provided by Eq. (2.2). We consider a rectangular structure occupying the studied domain $\Omega\subset\mathbf{R}^2$; $\Omega=(0,L)\times(0,l)$ with L and l are respectively its length and its width. The structure is fixed at left edge and submitted at the right edge to a load-dependant boundary condition δ. The upper and lower edges are free. We consider Dirichlet boundary conditions for damage variable α on the right and left edges of our structure which are given in the following equation:

$$\alpha(x_1=0,x_2)=\alpha(x_1=L,x_2)=0,\quad \forall x_2\in[0,l]. \tag{3.1}$$

The problem consists in finding the displacement satisfying:

$$\frac{\partial^2 u}{\partial x_1^2}+\frac{\partial^2 u}{\partial x_2^2}=0 \quad \text{dans} \quad \Omega, \tag{3.2a}$$

$$u(0,x_2)=0,\quad u(L,x_2)=\delta(t),\quad \forall x_2\in[0,1], \tag{3.2b}$$

$$\frac{\partial u}{\partial n}=0,\quad \forall(x_1,x_2)\in[0,L]\times[0,l]. \tag{3.2c}$$

A standard linear (P1) Lagrange finite element method was used to discretize the problem on u and α respectively in the following equations (Eqs. (3.3) and (3.4c)):

$$P(U)_\alpha\left\{\begin{array}{l}\text{Find } u;\ u\in\mathcal{A}_\delta \text{ as } \forall v\in\mathcal{A}_0:\\ \int_\Omega\big((1-\alpha)^2+\epsilon\big)\nabla u\cdot\nabla v d\Omega=0,\end{array}\right. \tag{3.3}$$

with:

$$\mathcal{A}_\delta = \{u \in H^1(\Omega) \text{ as } u = \delta \text{ in } \Gamma_1\}, \tag{3.4a}$$

$$\mathcal{A}_0 = \{v \in H^1(\Omega) \text{ as } v = 0 \text{ in } \Gamma_1\}, \tag{3.4b}$$

$$P(\alpha)_U = \begin{cases} \text{Find } \alpha;\ \alpha \in H^1(\Omega) \text{ as } \forall \beta \in H^1(\Omega): \\ \int_\Omega \alpha\beta|\nabla U|^2 d\Omega + \int_\Omega \frac{G_c}{2\eta}\alpha\beta d\Omega + \int_\Omega 2G_c\eta\nabla\alpha\cdot\nabla\beta = \int_\Omega \beta|\nabla u|^2 d\Omega. \end{cases} \tag{3.4c}$$

Eq. (3.3) gives the anti-plane displacement u. It will be injected in the Eq. (3.4c) to find the damage variable α.

The alternate minimizations algorithm is as follow:

Step 1 Require $\alpha(\delta=0)$, $d\delta = T/N$

Step 2 For $i=1$ to N do

Step 3 Set $\delta = id\delta$

Step 4 Find u solution of Eq. (3.3)

Step 5 Find α solution of Eq. (3.4c) with respect the irreversibility condition: $\alpha(\delta) \geq \alpha(\delta - d\delta)$

Step 6 End for

The material properties are $\mu=1$ and fracture toughness $G_c=1$. The mesh consists of approximately 11276 linear finite elements and 5789 nodes. The mesh size is $h=0.04$, the regularization parameters is $\eta=0.06$ and $\epsilon=10^{-5}$. We discretize the load interval $N=440$ in $d\delta=0.01$ equi-distributed load steps. Fig. 5 represents the evolution of damage field in

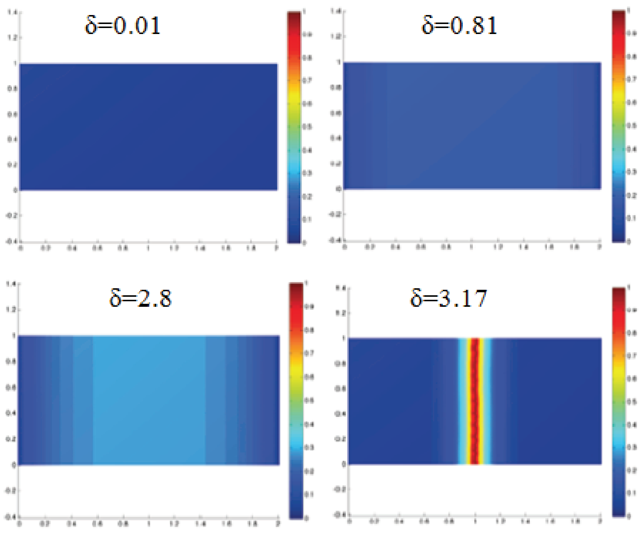

Figure 5: Crack propagation.

the rectangular domain as a function of load. A brutal cracking appears and the critical load is overestimated $\delta_c > \delta_c^{th} = 2$. In fact, for $L=2$, $G_c=1$ and $\mu=1$, the theoretical critical load δ_c^{th} is:

$$\delta_c^{th} = \sqrt{\frac{2LG_c}{\mu}}. \tag{3.5}$$

The alternate minimizations algorithm cannot expect to converge to the global minimizer of $E(U,\alpha)$. Those evolutions have to correspond to local minimizer of the regularized energy. Otherwise, the load causing fracture δ_c converges to the theoretical value when the ratio h/η decreases and converges to zero. Thus, if $\eta \gg h$, the surface energy converges to the theoretical value $E_{surf}^{th}=1$. We remind that Bourdin et al. [5] shows that the surface energy may be approximated using the following formula:

$$E_{surf} = G_c \int_\Omega \Big(\frac{\alpha^2}{4\eta} + \eta \nabla\alpha \nabla\alpha \Big) dx_1 dx_2 \simeq G_c \Big(1 + \frac{h}{4\eta} \Big) H^1(\Gamma), \tag{3.6}$$

where $H^1(\Gamma)$ is the length of crack. So, we amplify the fracture toughness by a factor $(1+h/4\eta)$, yielding an effective toughness $G_{eff} = G_c(1+h/4\eta)$ which has to be taken into account when interpreting the numerical results. So, we justify why in the last numerical computations, the surface energy E_{surf} is always superior to 1.

But, if $\eta \gg h$ and η tends to zero, the surface energy is $E_{surf} \simeq E_{surf}^{th} = 1$. So, the regularization parameter η should be chosen large enough, as compared to the discretization step h ($\eta \gg h$) and η must meet one of the $\Gamma-$*convergence* properties of regularized energy for the problem of brittle fracture ($\eta \ll 1$).

Moreover, we know that if the mesh is more tightened (mesh size h is so small), the obtained solution using the finite element method is accurate to the analytic solution. We model material failure using a gradient damage model characterized by the energy function $E(u,\alpha)$. We conclude that with a best choice of numerical parameters ($h \ll \eta \ll 1$), we simulate the crack propagation in brittle materials, like as glass and ceramic, using the alternate minimizations algorithm.

4 Thermo-Mechanical model of brittle fracture

We consider a rectangular piece with isotropic elastic stiffness tensor A_0 and thermal expansion coefficient β. The initial temperature is T_0, its lower edge is brought in contact with dry ice held at temperature T_s. Assuming a null flux through the lateral and superior edges of the domain and when the heat penetration depth is small compared to the length L. We neglect the effect of cracks on the heat transfer throughout the sample, and thermo-elastic effects, i.e., assume that the deformation is slow enough that it induces no changes in the temperature fields. These assumptions allow us to compare our numerical experiments with the experimental ones founded in literature. So, we compute

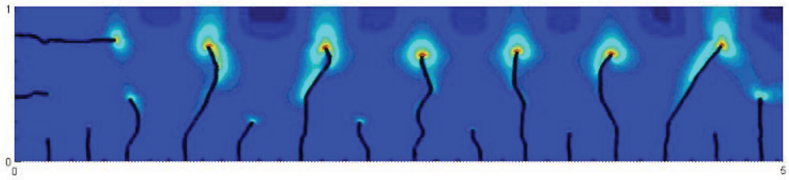

Figure 6: Numerical simulation of brittle material submitted to a thermal shock.

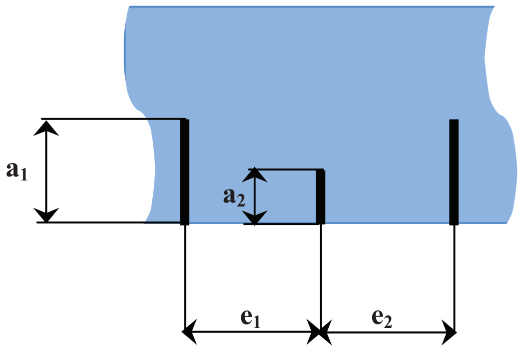

Figure 7: Thermal shock cracks pattern.

the temperature field at each time step, then minimize the total energy in which thermal expansion is accounted for by replacing the elastic term $P(e(u))$ in Eq. (1.1) with:

$$P(e(u),T) = \int A_0(e(u)-\beta T):(e(u)-\beta T)dx. \tag{4.1}$$

Fig. 6 represents the numerical simulation of a brittle material submitted to a thermal shock. We show only the damage field $(\alpha=1)$.

During the initial stage, the thermal shock cracks initiate and propagate uniformly, then the propagation speed decreases gradually with the release of thermal stress until the elastic energy E_{elast} cannot support the simultaneous propagation of all cracks. We defined a fundamental region with a minimum period, as shown in Fig. 7, where e_2 is the minimum crack spacing and a_2 is the crack length. When the minimum point of the surface energy E_{surf} jumps to a certain curve of spatial period doubling every time step dt, crack continues to propagate until a length of a_1, whereas the other cracks stop with a length of a_2 but always with an equal spacing $e_1=e_2$. This process can be repeated until the elastic energy induced by thermal stress cannot support the propagation of any cracks. The numerical simulations can conveniently reproduce the evolution of thermal shock cracks, which is difficult to observe experimentally. It was found that with an increase in the thermal shock temperature the initiating crack level appears between the developed crack levels; the length of the longest crack level continues to increase, whereas the other crack levels become shorter.

These interesting phenomena were experimentally confirmed as shown in [27]. In fact, we show in Fig. 8 the experimental results for the crack patterns founded by [27]

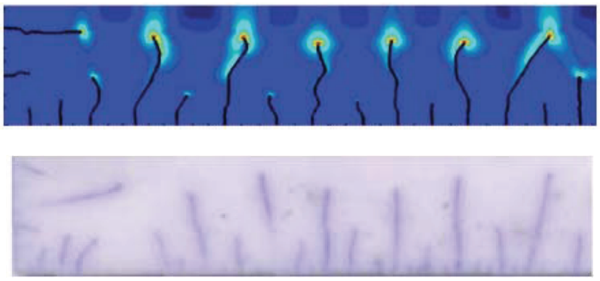

Figure 8: Comparison between the crack patterns in numerical models and in real specimen.

and the numerical ones. The simulations reproduce faithfully the crack patterns obtained from quenching test. The similarity between the numerical results and the real test is understood. So, the numerical study let us to understand the formation and the evolution of thermal shock crack patterns in brittle materials.

5 Modeling of chip formation using the behavior law of Johnson and Cook

The workpiece material properties have been modeled using the Johnson and Cook plasticity model (Eq. (5.1)).

$$\sigma_{eq}=[A+B\varepsilon^n]\Big[1+C\ln\Big(\frac{\dot{\varepsilon}}{\dot{\varepsilon}_0}\Big)\Big]\Big[1-\Big(\frac{T-T_{amb}}{T_f-T_{amb}}\Big)^m\Big]. \tag{5.1}$$

Johnson and Cook work material model is used for elastic plastic work deformations. The simulation results include not predicted chip formation. The Johnson-Cook law have a main apport in the cutting process. In fact, the domain of validity of the law of Johnson Cook covers the area of variation of plastic deformation (some units), rates of deformation (reaches the value $10^5\mathrm{s}^{-1}$) and temperature which can reach 60% of the melting temperature of the material in machining processes. The workpiece is modeled as a deformable rectangular solid, the length and the width are respectively L and l. The behavior law of the workpiece is defined by the Johnson Cook law. The material of the workpiece is the steel AISI1045 (C48 according to AFNOR standard). The coefficients of the constitutive law is presented in the Table 1.

On the other hand, several choices already exist in literature for the modeling of the cutting tool. We consider the cutting tool as a rigid material. The tool cutting edge radius

Table 1: The coefficients of the behavior law.

A	B	C	n	m	$\dot{\varepsilon}_0$	T_f(C)	T_{amb}(C)
800	700	0.04	0.5	1	1	1460	20

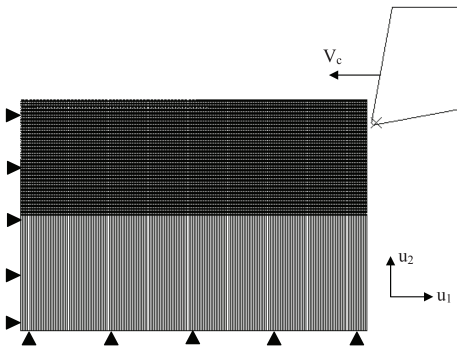

Figure 9: Cutting model.

is equal to 0.05mm. The rake and clearance angle are respectively equal to 10° and 11°. So, the cutting model is defined using ABAQUS is presented in Fig. 9.

The dimension of any element in the upper side of the workpiece is 0.05mm (according to $\overrightarrow{u_1}$) and 0.03mm (according to $\overrightarrow{u_2}$). Whereas, the dimensions are respectively equal to 0.05mm (according to $\overrightarrow{u_1}$) and 5mm (according to $\overrightarrow{u_2}$) in the lower side. A cutting speed V_c is applied on the tool and the lower and left edges of the workpiece are fixed. In the first, we show the formation of continuous chip in Figs. 10 and 11. They present respectively the variation of Von Mises stress and temperature in our structure. We simulate the continuous chip formation which is characterized by a plastic deformation process in the primary shear zone. We note in Figs. 10 and 11 that the Von Mises stress and the temperature are maximal in the primary shear zone. The maximal von Mises stress is : $\sigma^{\max}_{vonMises}=1800$MPa. The analysis of the thermal field during the simulation of the cutting shows that maximum temperature is located around the tool tip, $T^{\max}=839$°C. There is no separation criterion defined since chip formation is assumed to be due to plastic flow, therefore, the chip is formed by continuously remeshing the workpiece.

6 Mechanisms of discontinuous chip formation in hard machining

In this section, we use the same characteristics of the workpiece and the tool in the simulation of orthogonal cutting with continuous chip formation. Changes in the model of the last paragraph concern the mesh size of the workpiece, the cutting speed and the cutting thickness. The dimension of any element in the upper side of the workpiece is 0.035mm (according to $\overrightarrow{u_1}$) and 0.025mm (according to $\overrightarrow{u_2}$). The total displacement of the tool is 0.425mm. The cutting speed is $V_c=500$m/min and the cutting thickness is $h_1=1$mm. We present in the next two methods to simulate discontinuous chip using a procedure of deleting elements method and the thermo-Mechanical model of Johnson and Cook of ductile fracture.

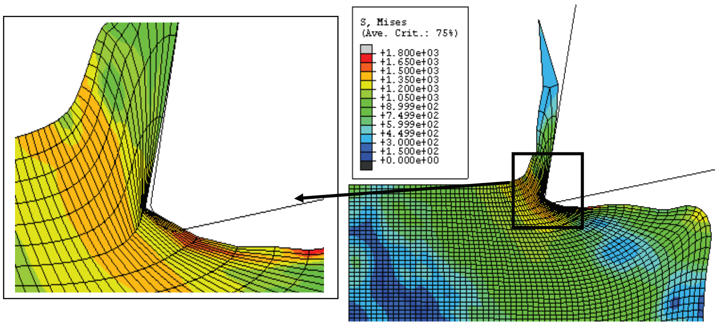

Figure 10: Variation of the Von Mises stress.

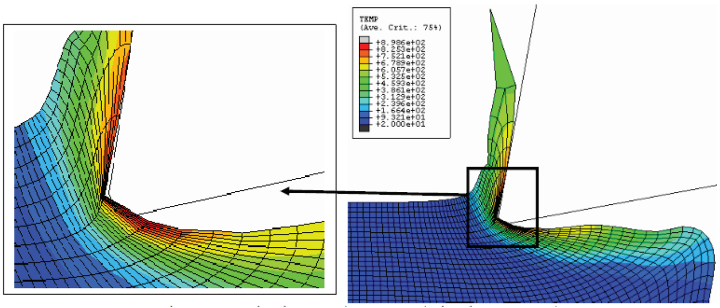

Figure 11: Variation of the temperature.

6.1 Procedure of deleting elements method

To simulate the initiation and propagation of cracks, we add a calculate module for the cyclic removal of the damaged elements during the simulation. Only a minority of work [35] succeeds in establishing this type of technique. The main idea is to intercept the intermediate results generated during the simulation to identify the damaged elements. Then, the model will be updated by removing damaged elements and the simulation will continue. This technique will be applied periodically during the simulation. Abaqus allows the exploitation of its outputs using external programs called subroutines which provides a strong and flexible analysis tool. Thus, a subroutine may access to a simulation outputs which are saved in a file generated after the simulation end. This file is composed of a set of records.

We present in Fig. 12 some examples of records which may exist in an output file. Records having as key value 107 define the node coordinates. Records having as key value 1900 represent the model elements defined by enumerating nodes constituting each element. Besides, records having as key value 101 represent the displacement of each node of the resulting model compared to the initial one along the different coordinate axes. The external module should be able to exploit the simulation outputs, updating the model, and to continue the simulation. We decomposed the real simulation time

Record key: 107 **Output variable identifier:** COORD
Record type: Coordinates
Attributes: **1 –** Node number.
2 – First coordinate.
3 – Second coordinate.
4 – Etc.

Record key: 1900 **Record type:** Element definitions
Attributes: **1 –** Element number.
2 – Element type (characters, A8 format, left justified).
3 – First node on the element.
4 – Second node on the element.
5 – Etc.

Record key: 101 **Output variable identifier:** U
Record type: Displacements
Attributes: **1 –** Node number.
2 – First component of displacement.
3 – Second component of displacement.
4 – Etc.

Figure 12: Structure of the output records of Abaqus.

into a set of periods. We use this period as a partial simulation time having as result an intermediary result of the real simulation. After each partial simulation, the removal material module is executed in order to generate a new model which will be used as input of the next partial simulation. The generated model corresponds exactly to the model resulting of the previous simulation but where the damaged elements are removed.

The removal materials model is presented in Fig. 13. This module takes as input a file describing the initial model and begins by starting the first partial simulation which generates an output file. The latter will be converted by our external module to generate a file which will be used by the Fortran subroutine. Then, the materials removal module will run the Fortran subroutine which will use the converted file as well as files describing the geometry of the model resulting from the previous partial simulation. The latter includes the piece nodes and elements, and the cutting tool nodes and elements.

Thus, the Fortran subroutines will use these data in order to generates files describing the geometry of the new model resulting from the partial simulation as well as the stress and deformation of each element of the model. Based on these data, the material removal module will identify elements which should be deleted. Then, it will generate the new model which corresponds to the new geometry where damaged elements are deleted, and finally apply the resulting stress and deformation as initial conditions of the new model. The latter will be used as input of the next partial simulation.

In order to identify the elements which should be deleted, the material removal module analyzes the Fortran subroutine output to select elements having a MISES value higher than the tensile strength of the used material.

Thus, element 2 (Fig. 14) is deleted when its equivalent von Mises constraint reaches the tensile strength. The new model allowing the execution of the next partial simulation is created while respecting the following constraints:

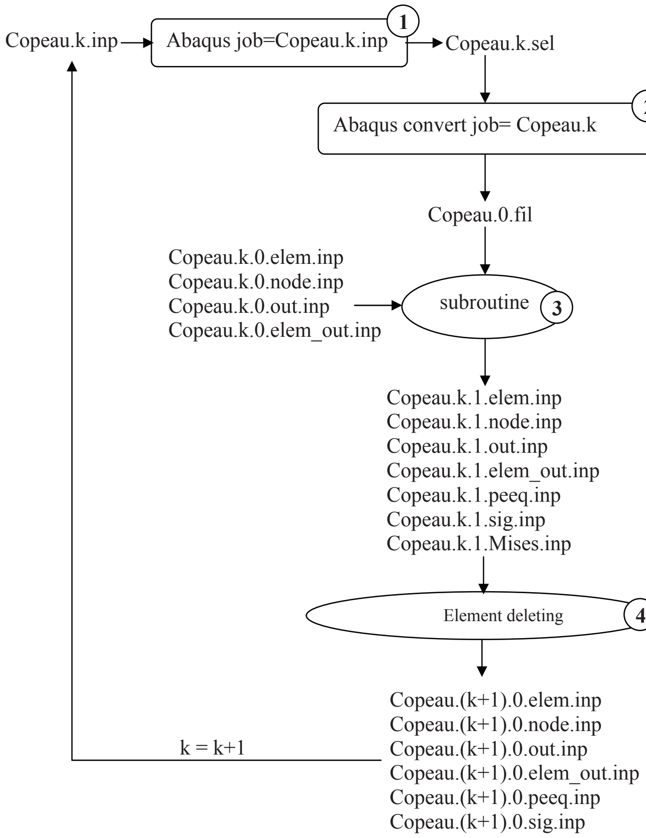

Figure 13: Material removal process.

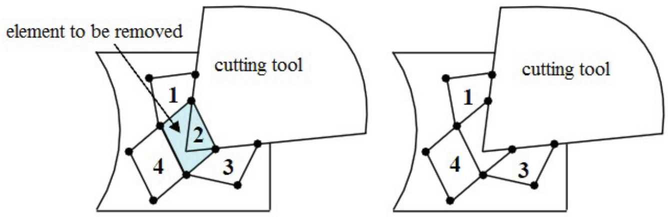

Figure 14: Elements removal principal.

- The nodes coordinate of the new model correspond to the coordinates generated by the subroutine. Thus the geometry of the new model corresponds to the geometry of the model resulting from the previous partial simulation
- A crack is initiated and the element, which the Von Mises stress became higher then the critical value, is deleted along with all parameters related to this element including element connectivity definition, the strain value and the stress value.
- For each element of the new model, initial conditions specifying the values of $PEEQ$,

TEMP, and *S* should be added in order to ensure that the initial values of these parameters for the next partial simulation correspond to their values at the end of the previous partial simulation. Thus, we ensure a correct evolution of these parameters values during the real simulation.

Based on this method, we represent in Fig. 15 first iteration and in Fig. 16 the final chip formation and separation during the process. So, every element having an equivalent Von Mises stress value $\sigma_{vonMises}$ higher than according to the tensile strength $\sigma_r = 750$MPa will be removed.

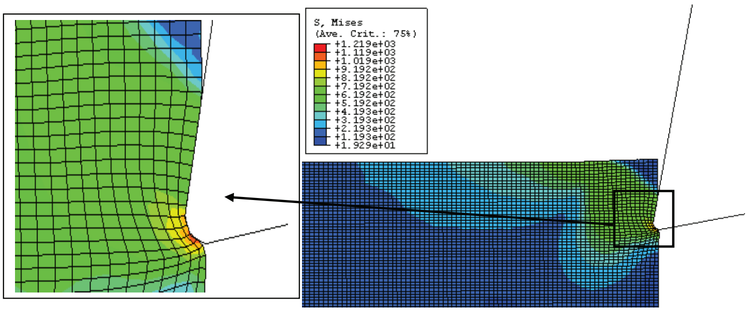

Figure 15: First iteration.

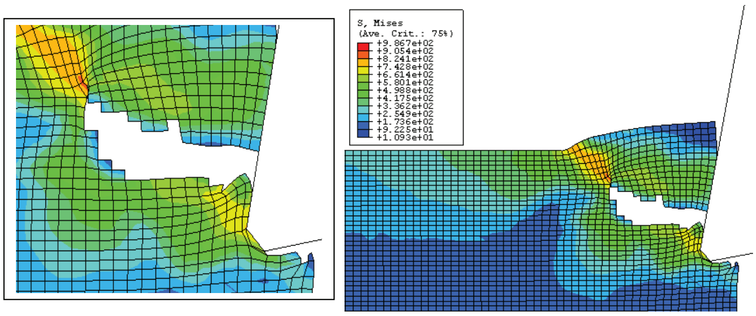

Figure 16: Final iteration.

The maximal equivalent Von Mises constraint is $\sigma_{\max} = 986$MPa. We notice that the equivalent Von Mises constraints in the piece are maximal in the primary shear zone. If we continue the simulation, the first chip fragment will be totally detached of the piece and a second chip fragment will be formed.

6.2 Thermo-Mechanical model of ductile fracture

Johnson and Cook [6] proposed a model for metals subjected to strains, strain rates and heating effects. In this model, the von Mises flow stress is depending on strain, strain rate sensitivity and temperature dependence of stress. They proposed also a damage criterion

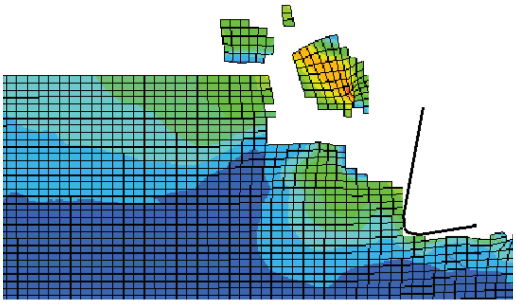

Figure 17: Discontinuous chip formation based on the Johnson and Cook damage law.

based on cumulative plastic strain and given by Eqs. (6.1a) and (6.1b).

$$\varepsilon_r = \left[D_1 + D_2 \exp\left(D_3 \frac{\sigma_H}{\sigma_{eq}}\right)\right]\left[1 + D_4 \ln\left(\frac{\dot{\varepsilon_{eq}}}{\dot{\varepsilon}_0}\right)\right]\left[1 + D_5\left(\frac{T - T_{amb}}{T_f - T_{amb}}\right)^m\right], \tag{6.1a}$$

$$W_{JC} = \sum \frac{\Delta\varepsilon_{eq}}{\varepsilon_r}. \tag{6.1b}$$

In Eq. (6.1a), σ_H is the hydrostatic stress, σ_{eq} is the von Mises equivalent stress, $\dot{\varepsilon}_0 = 1\text{s}^{-1}$ is the reference strain rate. D_1, D_2, D_3, D_4 and D_5 are the material constants. In Eq. (6.1b), $\Delta\varepsilon_{eq}$ is the increment of equivalent plastic strain. So, the fracture will occur when $W_{JC} = 1$, the stresses are set to zero, simulating rupture. The problem of this model is the identification of its parameters (D_1 to D_5).

The material data are given in Table 2 and will be used in numerical computation. They may be given from the literature [36] and determined also experimentally.

Based on this method, we represent in Fig. 17 some discontinuous chip which are formed by using the Johnson and Cook damage law.

We can show the coefficients of the Johnson and Cook damage law have an important influence on the morphologie of chip and the value of plastic strain. The problem of this model is the identification of its parameters (D_1 to D_5). So the actual research problem is to define a method to identify the Johnson Cook behavior and damage laws coefficients. To achieve this purpose, we can employ an orthogonal cutting simulation by the continuous chip formation. The criteria of identification take into account both the geometry of the chip, the variation of temperature and the cutting forces, and these results may be compared to the experimental ones.

Table 2: The coefficients of the Johnson and Cook damage law.

D_1	D_2	D_3	D_4	D_5
0.3	0.28	-3.03	0.0014	1.12

7 Conclusions

In this paper, we propose in the first, numerical method to simulate the crack propagation in a brittle and ductile materials.

In fact, this work deals with two problems. The first consists of 2D anti-plane shear experiment on a rectangular domain and without an initial crack. The second one consists of presenting a cracking process in ceramic materials under thermal shock. The numerical simulations reveal the periodical and hierarchical characteristics of thermal shock cracks. So, we can simulate the crack propagation in brittle materials using a damage thermo-mechanical model. The last is the variational approach based on the theory of Griffith.

In the second, we present numerical implementation of thermo-mechanical model used to simulate the cutting process of ductile materials. We use the Johnson and Cook laws of behavior and damage to simulate the formation of continuous and discontinuous chips.

In fact, the Johnson and Cook law is used to model the workpiece behavior. Thus, we simulate the formation of discontinuous chip. It is characterized by its periodic rupture. The shear stress reaches the breaking point of the material in the primary shear zone and a crack propagates. The discontinuous chip is obtained by using two methods, the element deletion criterion and the failure model of Johnson and Cook.

Acknowledgements

This research was supported by the Tunisian Chemical Groupa and by the LSPM Laboratory, University of Paris 13, Villetaneuse, France. Helpful discussions with Radhi Abdelmoula are gratefully acknowledged.

References

[1] A. Griffith, *The phenomena of rupture and flow in solids*, Philosophical Transactions of the Royal Society of London, 221 (1921), pp. 163–198.
[2] B. Bourdin, The Variational Approach to Fracture, PhD thesis, University Paris 13, 1998.
[3] G. Francfort and J. J. Marigo, *Vers une théorie énergétique de la rupture fragile,* Comptes Rendus Mécanique, 330 (2002), pp. 225–233.
[4] B. Bourdin, G. Francfort and J. J. Marigo, *Numerical experiments in revisited brittle fracture*, J. Mech. Phys. Solids, 48(4) (2000), pp. 797–826.
[5] B. Bourdin, G. Francfort and J. J. Marigo, *The variational approach to fracture*, J. Elasticity, 91 (2008), pp. 5–148.
[6] G. R. Johnson and W. H. Cook, *A constitutive model and data for metals subjected to large strains, high strain rate, and temperatures,* Proceedings of the 7th International Symposium on Ballistics, The Hague, Netherlands, pp. 541–547, 1983.

[7] K. W. KIM, W. Y. LEE AND H. C. SIN, *A finite element analysis of machining with the tool edge considered*, J. Mater. Process. Tech., 86 (1999), pp. 45–55.

[8] T. OZEL AND E. ZEREN, *Fe modelling of stresses induced by high speed machining with round cutting tools,* 2005.

[9] T. OZEL AND E. ZEREN, *A methodology to determine work material flow stress and tool-chip interfacial friction properties by using analysis of machining*, J. Manufact. Sci. Eng., 128 (2006), pp. 119–129.

[10] T. OZEL, *Modelling of hard machining: effect of insert edge preparation in cbn cutting tools*, J. Mater. Process. Tech., 141 (2003), pp. 284–293.

[11] H. FASSI, L. BOUSSHINE, A. CHAABA AND A. ELHARIF, *Numerical simulation of orthogonal cutting by incremental elastoplastic analysis and finite element method*, J. Mater. Process. Tech., 141 (2003), pp. 181–188.

[12] J. L. ALCARAZ, I. LORENZO AND L. N. LACALLE, *Thermomechanical analysis of a chip machining process*, in: ABAQUS Users' Conference, 2003.

[13] H. BIL, S. E. KILIC AND A. E. TEKKAYA, *A comparison of orthogonal cutting data from experiments with three different finite element models*, Int. J. Machine Tools Manufacture, 44 (2004), pp. 933–944.

[14] M. BARGE, H. HAMDI, J. RECH AND J. M. BERGHEAU, *Numerical modelling of orthogonal cutting: influence of numerical parameters*, J. Mater. Process. Tech., 164-165 (2005), pp. 1148–1153.

[15] G. FRANCFORT AND J. J. MARIGO, *Revisiting brittle fracture as an energy minimization problem*, J. Mech. Phys. Solids, 46 (1998), pp. 1319–1342.

[16] G. E. OLEAGA, *On the path of a quasi static crack in mode iii*, J. Elasticity, 76 (2004), pp. 163–189.

[17] H. AMOR, J. J. MARIGO AND C. MAURINI, *Regularized formulation of the variational brittle fracture with unilateral contact: Numerical experiments*, J. Mech. Phys. Solids, 57 (2009), pp. 1209–1229.

[18] K. PHAM AND J. J. MARIGO, *Approche variationnelle de l'endommagement: I. les concepts fondamentaux*, Comptes Rendus Mécanique, 338 (2010), pp. 191–198.

[19] K. PHAM AND J. J. MARIGO, *Approche variationnelle de l'endommagement: Ii. les modèles à gradient*, Comptes Rendus Mécanique, 338 (2010), pp. 199–206.

[20] M. BULIGA, *Energy minimizing brittle crack propagation*, J. Elasticity, 52(3) (1998), pp. 201–238.

[21] M. CHARLOTTE, G. FRANCFORT, J. J. MARIGO AND L. TRUSKINOVSKI, *Revisiting brittle fracture as an energy minimization problem comparisons of griffith and barenblatt surface energy models,* In: Symposium on Continuous Damage and Fracture, 2000.

[22] L. AMBROSIO AND V. M. TORTORELLI, *Approximation of functionals depending on jumps by elliptic functionals via gamma-convergence*, In: Commun. Pure Appl. Math., 43 (1990), pp. 999–1036.

[23] L. AMBROSIO AND V. M. TORTORELLI, *On the approximation of free discontinuity problems*, In: Boll. Un. Mat. Ital., B(7)6(1) (1992), pp. 105–123.

[24] D. MUMFORD AND J. SHAH, *Optimal approximations by piecewise smooth functions and associated variational problems*, In: Commun. Pure Appl. Math., XLII (1989), pp. 577–685.

[25] E. JAGLA, *Stable propagation of an ordered array of cracks during directional drying*, Phys. Rev. E, 2002.

[26] D. JENKINS, *Optimal spacing and penetration of cracks in a shrinking slab*, Phys. Rev. E, 2005.

[27] C. P. JIANG, X. F. WUA, J. LI, F. SONG, Y. F. SHAO, X. H. XU AND P. YAN, *A study of the mechanism of formation and numerical simulations of crack patterns in ceramics subjected to thermal shock*, Acta Mater., 60 (2012), pp. 4540–4550.

[28] B. BOURDIN, C. MAURINI AND M. KNEPLEY, *Numerical simulation of reservoir stimulation-a variational approach*, In: PROCEEDINGS, Thirty-Sixth Workshop on Geothermal Reservoir Engineering Stanford University, Stanford, California, January 31-February 2, 2011.

[29] A. GURSON, *Continuum theory of ductile rupture by void nucleation and growth: Part I-Yield criteria and flow rules for porous ductile media,* J. Eng. Mat. Tech., 99 (1977), pp. 2–15.

[30] V. TVERGAARD AND A. NEEDLEMAN, *Analysis of cup cone fracture in a round tensile bar,* Acta Metall., 32 (1984), pp. 157–169.

[31] J. LEMAITRE, Course on Damage Mechanics, Springer, Second Edition, 1991.

[32] V. LEMIALE, S. MEUNIER AND P. PICART, *Etude experimentale et numerique du decoupage de toles en faible epaisseur,* XV Congres de Mecanique, Nancy, Sept 2001, pp. 440.

[33] D. UMBRELLO, R. M'SAOOUBI AND J. C. OUTEIRO, *The influence of johnson-cook material constants on finite element simulation of machining of aisi 316l steel*, Int. J. Mach. Tool Manufacture, 47 (2007), pp. 462–470.

[34] NY. B. GUO, *A fem study on mechanisms of discontinuous chip formation in hard machining*, J. Mater. Process. Tech., 155-156 (2004), pp. 1350–1356.

[35] P. LESTRIEZ, Modlisation Numerique du Couplage Thermo Mcanique Endommagement en Transformation Finies, Application la Mise en Forme, PhD thesis, 2003.

[36] C. POIZAT, L. CAMPAGNA, L. DARIDON, S. AHZI, C. HUSSON AND L. MERLE, *Modeling and simulation of thin sheet blanking using damage and rupture criteria*, Int. J. Form. Process., 8(1) (2005), pp. 29–47.